

## Original Article

# 3D micro CT imaging of the human peripheral nerve fascicle

Liwei Yan\*, Jian Qi\*, Shuang Zhu, Tao Lin, Xiang Zhou, Xiaolin Liu

Department of Microsurgery and Orthopaedic Trauma, The First Affiliated Hospital of Sun Yat-sen University, Guangzhou, P. R. China. \*Equal Contributors.

Received July 8, 2016; Accepted April 25, 2017; Epub July 15, 2017; Published July 30, 2017

**Abstract:** Autologous nerve grafting is the gold standard for the treatment of peripheral nerve injury; however, it involves certain complications. With the maturity of three-dimensional (3D) bioprinting techniques, the 3D bioprinting of nerve grafts has become theoretically feasible. The primary 3D bioprinting of nerve grafts results in a 3D nerve structure, in particular, a fascicular 3D structure. The aim of this study was to identify a method for enhancing X-ray micro computed tomography (CT) to reconstruct 3D nerve structures. Here, we used three techniques, Lugol's iodine solution ( $I_2KI$ ) enhancement, calcium chloride enhancement and freeze-drying (n=6), to identify a better method for obtaining high-resolution 3D images of a normal human peripheral nerve fascicle. Contrast differences were employed to compare the homologous nerve structure with the fascicular structure in each group. Unlike hematoxylin and eosin (H&E) staining and scanning electron microscopy (SEM), the micro CT approach produced continuous serial images, which are necessary for 3D reconstruction. The fascicular increases in the contrast levels were  $211.74\pm 31.44\%$ ,  $-6.51\pm 1.46\%$  and  $125.41\pm 27.14\%$  for the H&E, SEM and micro CT methods, respectively. The calcium chloride enhancement resulted in an excellent contrast between the human nerve fascicle and the following tissues: the perineurium, connective tissue, epineurium, and endoneurium ( $P<0.001$ ). These findings indicate that the anatomical structures were clearly identified. This is the first use of micro CT to reconstruct a 3D image of a human peripheral nerve fascicle using three different pretreatment methods. Compared to H&E and SEM, our micro CT approach has the advantage of continuous serial imaging. In addition, compared to the iodine enhancement and freeze-drying methods, the calcium chloride-enhanced contrast method for micro CT scanning yielded the highest-quality 3D images of a human peripheral nerve fascicle.

**Keywords:** Human peripheral nerve fascicle, micro CT, Lugol's iodine solution ( $I_2KI$ ), calcium chloride, freeze-drying, 3D bioprinting

## Introduction

Peripheral nerve injury (PNI) always causes a considerable loss of sensory and motor functions in the innervated area, leading to a decreased quality of life. Although microsurgical techniques have improved, the results of surgical repair remain less than ideal [1]. Autologous nerve grafting is commonly used as the gold standard for nerve reconstruction, but autografts require additional surgery and lead to nerve loss without complete functional restoration [2-4]. Our group has shown that nerve repair is functionally possible using acellular nerve allografts (ANAs), which are derived from native peripheral nerves, retain the structure and extracellular matrix components of the

original nerve, and stimulate a minimal host immune response to connect gaps in the nerve [5-7]. ANAs are good candidates for nerve repair, but the clinical outcome of grafting is not always satisfactory. As three-dimensional (3D) bioprinting has become more widely available, printing nerve grafts has become more feasible. The main steps of the bioprinting process are imaging and design, selecting materials and cells, and printing the tissue construct [8]. To complete 3D bioprinting, we must first have a normal human 3D fascicular structure [9, 10].

Traditional histopathology (e.g., hematoxylin and eosin (H&E) staining) and scanning electron microscopy (SEM) allow for very high-resolution imaging of planes from tissue sections

## 3D micro CT of the nerve fascicle

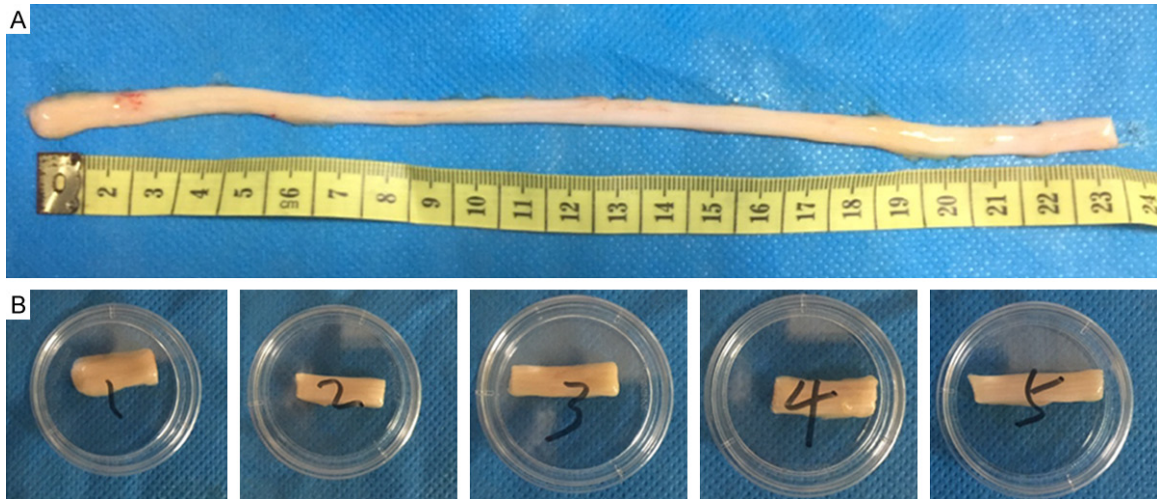


**Figure 1.** A: A 23-cm-long, fresh human tibial nerve from the lower limb of an amputation patient. B: The nerve was divided into 5 portions, each of which was 4 cm long. Segments 1, 2, and 3 were pretreated for micro CT with Lugol's iodine solution ( $I_2KI$ ), calcium chloride, and freeze-drying, respectively. Segment 4 was pretreated for H&E staining, and segment 5 was pretreated for SEM.

using specific staining methods. However, these methods are destructive and can only be used for two-dimensional (2D) imaging. A 3D image is difficult to obtain with these approaches because the sectioning and mounting processes often result in geometric nerve distortion. In addition, the staining process is time consuming and labor intensive. X-ray micro computed tomography (micro CT) can be used for the non-destructive analyses of tissue specimens. Micro CT was first introduced in the 1980s by Elliotte and Dorer and uses X-ray attenuation data acquired from multiple projection angles to produce high-resolution images. Micro CT uses X-rays to produce image files that can be compiled to generate 3D images [11]. Micro CT has non-destructive and reconstructive characteristics and can be used to analyze 3D tissue structures, particularly mineralized tissue, such as bone, teeth and cartilage [12-15]. Although micro CT is already an established technology for imaging different types of mineralized tissues, such as bone and teeth, soft-tissue applications of micro CT imaging in comparative morphology have been limited by low intrinsic X-ray contrast, particularly in peripheral nerves. With the use of certain contrast staining methods, micro CT can produce high-quality, high-resolution images of soft tissues [16]. Micro CT can be used to visualize fine soft-tissue details in embryos and invertebrates by increasing the differential attenuation of the X-rays [17, 18].

Thus, we investigated the use of 3D micro CT for the non-invasive characterization of the human fascicle. The aim of this study was to determine whether treating human peripheral nerve tissue with a micro CT contrast agent (i.e., Lugol's iodine solution ( $I_2KI$ ), calcium chloride or freeze-drying) can yield images with useful anatomical contrast compared to those obtained by H&E staining and SEM. In addition, we wanted to evaluate the most effective methods for micro CT scanning.

### Materials and methods

#### Human nerves

For this study, we used human tibial nerves excised from the lower limbs of amputation patients at The First Affiliated Hospital of Sun Yat-sen University. Each tibial nerve was 23 cm in length. External debris such as muscle and fat was removed. Fresh nerves were divided into 5 parts, each of which was 4 cm long, taking into consideration the elastic quality of fresh nerves (**Figure 1**). The fresh nerves were immediately fixed with 4% paraformaldehyde at room temperature for 4 hours and underwent the corresponding treatments for micro CT, H&E or SEM.

All procedures were performed with informed consent and were approved by the institutional review boards of the contributing institutions of The First Affiliated Hospital of Sun Yat-sen

## 3D micro CT of the nerve fascicle

University, in accordance with the Declaration of Helsinki.

### *Micro CT scanning and specimen fixation and staining*

All of the nerves were imaged with a micro CT system (Micro CT 80 SCANCO Medical, Basserdorf, Switzerland). The nerves were prepared for their respective methods and placed in a sample holder for imaging. A sagittal scout image, comparable to a conventional planar X-ray, was obtained to define the starting and ending points for the acquisition of a series of coronal slices through the nerve. The nerves were imaged with foam, which does not block X-rays, as the background medium. Images were generated by operating the X-ray tube at a voltage of 55 kVp and a current of 72  $\mu$ A. The total acquisition time was 36 min per sample, and 216 slices were obtained for each scan. Images were obtained at an isotropic resolution of 5  $\mu$ m for the nerve scan.

### *Lugol's iodine solution ( $I_2/KI$ ) enhancement method*

Fresh nerves were immersed in 4% paraformaldehyde for approximately 12 hours. In the iodine-enhancing process, the nerves were first removed from the 4% paraformaldehyde solution and then washed in distilled water for 4 hours at room temperature. The nerves were then immersed in Lugol's iodine solution (Sigma-Aldrich, St. Louis, USA) diluted to 50% using distilled water and shocked (oscillation frequency of 120 GHz per hour) for 24 hours. Finally, filter paper was used to absorb water from the nerve surfaces in preparation for scanning.

### *Calcium chloride enhancement method*

Fresh nerves were immersed in 4% paraformaldehyde for approximately 12 hours. The first step of the calcium chloride enhancement process was similar to that of the iodine enhancement process. Subsequently, the nerves were immersed in a saturated calcium chloride (Sigma-Aldrich, USA) solution ( $CaCl_2$  in distilled water with no visible material at the bottom) and shocked for 24 hours (oscillation frequency of 120 GHz per hour). The final step of this process was similar to that of the iodine enhancement process.

### *Freeze-drying method*

Fresh nerves were immersed in 4% paraformaldehyde for approximately 12 hours. The first step of the freeze-drying process was similar to that of the iodine enhancement process. The nerves were then immersed in liquid nitrogen and placed in a lyophilizer for 7 days to remove water molecules.

### *H&E staining*

For histological analysis, nerves were fixed in 4% paraformaldehyde for 2 hours, followed by several washes in phosphate-buffered saline (PBS) for 24 hours. The fixed nerves were dehydrated by a graded series of ethanol, embedded in paraffin wax, sectioned to a thickness of 8  $\mu$ m, and mounted on microscope slides. Sections were stained with H&E to visualize the transverse structure of the nerves.

### *SEM*

Nerves were fixed in 4% paraformaldehyde for 2 hours, washed in PBS for 24 hours and snap-frozen by immersion in liquid nitrogen. The fixed nerves were dehydrated by a graded series of ethanol (10 to 100%), followed by critical-point drying with  $CO_2$ . After the samples were mounted with carbon cement and sputter-coated with an approximately 10-nm-thick gold film, they were examined by SEM (FEI QUANTA 200, Netherlands) using a lens detector with a 5-kV acceleration voltage at calibrated magnifications. Transverse sections of the nerve segments were analyzed.

### *Quantification of the nerve brightness and contrast levels*

To test which method yielded the greatest levels of contrast between fascicular and connective tissue via micro CT imaging, we quantified the pixel brightness using grayscale values (GVs) from 0 (black) to 255 (white). First, we used a DICOM viewer (SANTE DICOM Viewer, Germany) to convert the DICOM images to TIFF images, removing all background media (i.e., foam) from the single-slice TIFF images. Second, the resultant image files containing only nerve information were opened in Adobe Photoshop (Adobe Systems, Mountain View, CA, USA) to measure the pixel brightness. Specifically, the mean  $GV \pm$  standard deviation (SD) for each

## 3D micro CT of the nerve fascicle

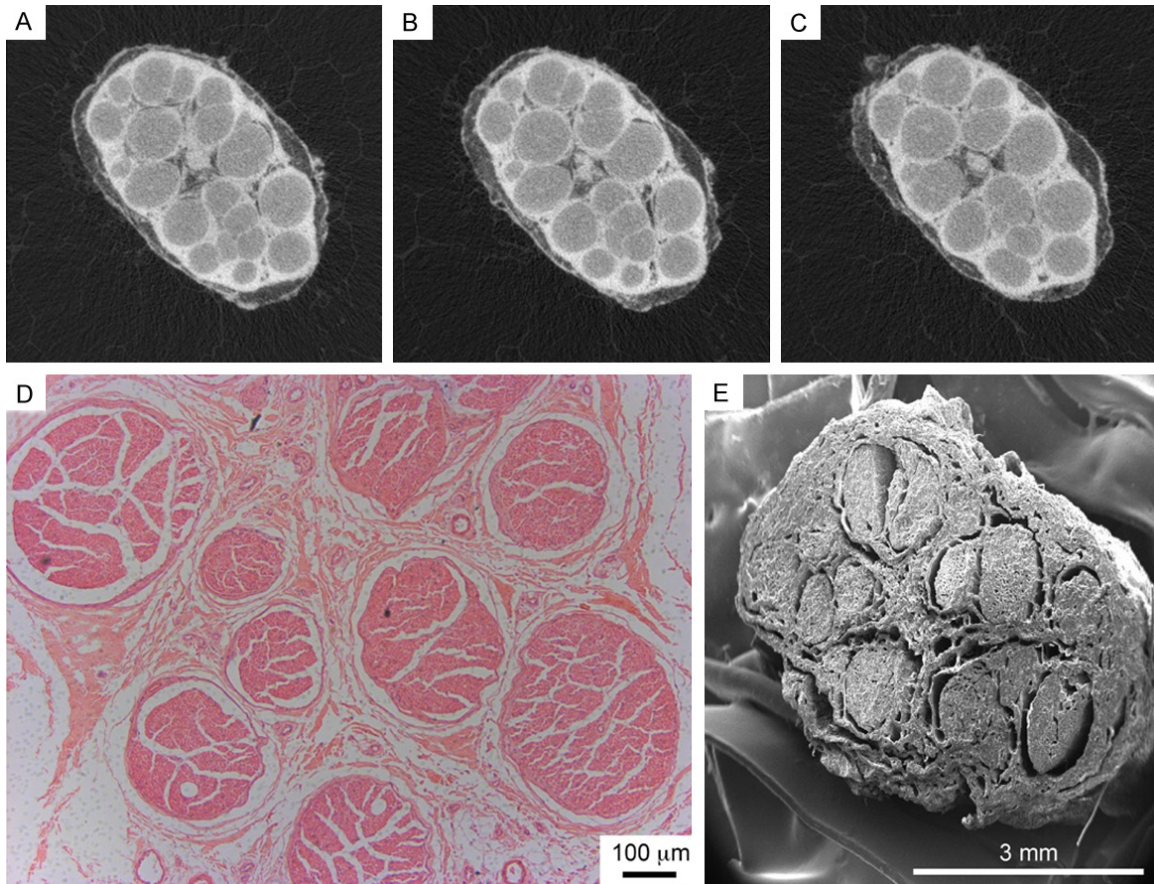


**Figure 2.** The three methods yielded images generally comparable with those obtained by H&E and SEM. Micro CT yields continuous serial images, while H&E and SEM only yield intermittent images.

5×5 pixel square sampled within the anatomical structures was obtained using the histogram tool in Adobe Photoshop for each complete micro CT TIFF image. Adobe Photoshop automatically calculated the mean GV and corresponding SD for each square of sampled pixels. To determine the characteristic GV for each method, the mean values of all pixel samples of the homologous nerve under the same staining regime were averaged. Pooled SDs for these means were then calculated by squaring each SD to derive the variance, averaging the variances for similar tissues at similar staining durations, and taking the square root of those averaged variances [19]. Finally, the contrast level of each method was determined using the following equation:  $c = \frac{Xt - X_{mean}}{X_{mean}}$ , where C is the contrast difference as a percentage, Xt is the mean GV of the structure for a given nerve, and Xmean is the mean GV for the entire TIFF slice. Contrast difference is a unitless measure and

is represented here as a percentage value compared to the mean brightness of the entire corresponding TIFF image. Positive values were brighter than the mean, and negative values were darker. Comparing contrast levels in this way allowed us to determine whether certain tissues are more clearly visualized under certain preparation regimes. No adjustments were made to the brightness or contrast levels of the frontal-view TIFF images prior to taking these measurements.

### *Statistical analysis*

All of the numerical data are presented as the means and SDs. Student's t-test was used to test the statistical significance of differences between sample means. All of the results were subjected to statistical analysis using SPSS v11.5 software for Windows (student version). Statistically significant values were defined as  $P < 0.01$ .

## 3D micro CT of the nerve fascicle

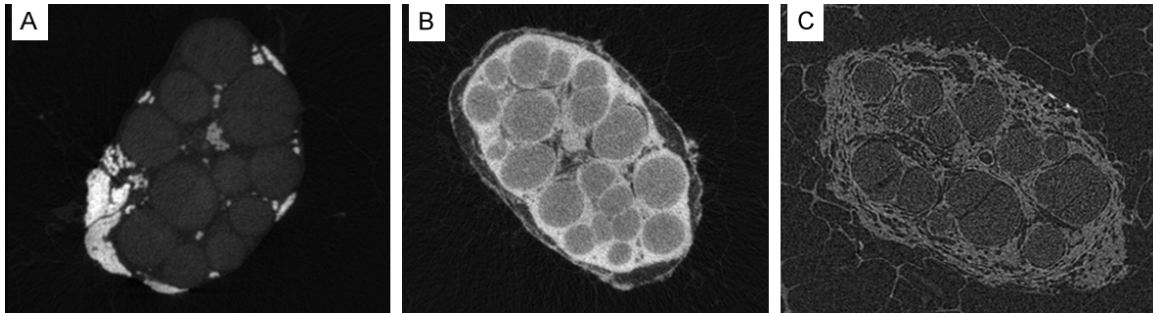


**Figure 3.** 2D coronal sections of 3D micro CT images of normal human nerves treated by different methods. From left to right, the contrast is enhanced by (A) Lugol's iodine solution ( $I_2KI$ ); (B) Calcium chloride; and (C) freeze-drying. There is no native micro CT scan of the normal nerve without a pretreatment. (A) The iodine enhancement method yielded the highest-quality images of the connective tissue and fascicle; (B) The calcium chloride enhancement method produced the highest-quality images of the perineurium, connective tissue and fascicle; and (C) the freeze-drying method damaged the perineurium structure.

### 3D reconstruction

The gross anatomical structures of the normal human nerve, including the epineurium, connective tissue, perineurium, and fascicle, were reconstructed digitally using Avizo software (Visualization Sciences Group, Burlington, MA, USA) on an iMac (Apple). The anatomical relationships of these structures were then verified using previous studies in the literature and standard gross dissection techniques.

### Results

In this study, we had to consider that nerves are elastic. **Figure 1** shows a fresh human tibial nerve 23 cm in length. However, when the nerve was divided into 5 parts, each part was approximately 4 cm long. This phenomenon indicates that micro CT images of these nerves will show sizes somewhat different from those of normal nerves.

Previous results showed that H&E and SEM can achieve very high-resolution images of tissue sections (**Figure 2D, 2E**). In our results, micro CT yielded comparable-quality images of the connective tissue, epineurium endoneurium and fascicle; however, H&E could not reveal fully detailed images. Furthermore, micro CT yielded continuous serial images, whereas H&E and SEM only yielded intermittent images (**Figure 2A-C**).

Next, we attempted to determine which method could yield an image ideal for 3D reconstruction. The results showed that the iodine enhancement method produced relative-

ly high-quality images of the connective tissue and fascicle (**Figure 3A**). The calcium chloride enhancement method yielded the highest-quality images of the perineurium, connective tissue and fascicle (**Figure 3B**). **Figure 3C** illustrates that the freeze-drying method damaged the perineurium structure.

Using tomography and contrast, the five major homologous nerve structures could be clearly identified using the different methods (**Figure 4**). The endoneurium has enclosed nerve fibers bundled into groups and forms the most important microstructure, called the nerve fascicle. In our endoneurium imaging findings, all three methods showed comparable results with H&E; however, the freeze-drying method yielded high-quality images of the endoneurium (**Figure 4E**).

Using C values, we attempted to quantify the contrast difference of each homologous nerve structure obtained using the different methods. We found that for the fascicle, the three methods showed contrast levels of  $211.74 \pm 31.44\%$ ,  $-6.51 \pm 1.46\%$  and  $125.41 \pm 27.14\%$ . Comparing the perineurium, connective tissue, and epineurium endoneurium with the fascicle, our results demonstrated that the C values were significantly different ( $P < 0.001$ ) when the calcium chloride enhancement method was used (**Table 1**), indicating that the calcium chloride-enhanced images were more recognizable.

A normal human 3D fascicular structure is necessary to complete 3D bioprinting. We used the calcium chloride enhancement method to re-

## 3D micro CT of the nerve fascicle

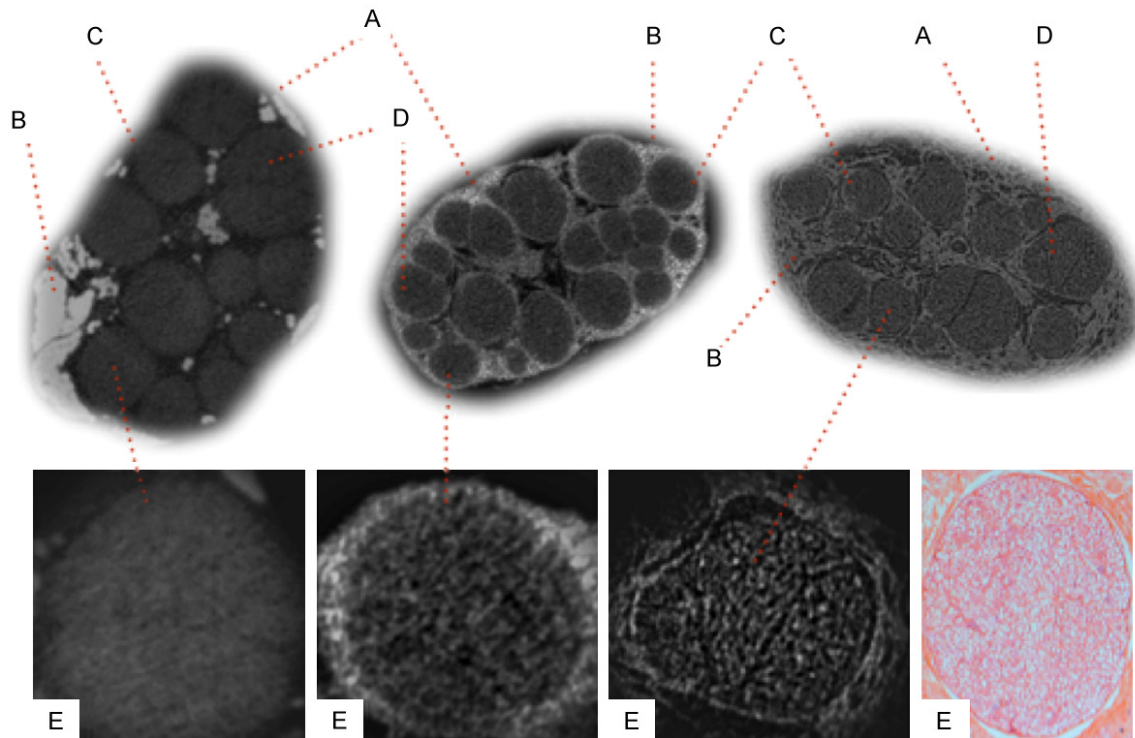


**Figure 4.** All three methods showed the anatomical structure of the (A) perineurium, (B) connective tissue, (C) epineurium, (D) fascicle and (E) endoneurium. From left to right, the results for the treatments with Lugol's iodine solution ( $I_2KI$ ), calcium chloride, and H&E are shown.

**Table 1.** Comparison of the fascicle with other homologous nerve structures using different methods

Methods	C-fascicle	C-perineurium (p)	C-connective tissue (p)	C-epineurium (p)	C-endoneurium (p)
Iodine	211.74±31.44	247.28±39.29 (P=0.082)	-16.53±3.01 (P=4.56E-06)	226.70±69.45 (P=0.731)	256.47±46.56 (P=0.059)
Calcium chloride	-6.51±1.46	45.14±11.46 (P=4.82E-05)	-59.72±7.66 (P=3.18E-06)	-21.92±6.38 (P=5.88E-04)	16.91±3.88 (P=2.22E-06)
Freeze-drying	125.41±27.14	133.99±25.40 (P=0.513)	104.81±28.66 (P=0.162)	119.41±31.01 (P=0.659)	131.31±30.02 (P=0.706)

Contrast differences obtained using different methods. For all values, n=6. Iodine refers to the Lugol's iodine solution ( $I_2KI$ ) enhancement method. Calcium chloride refers to the calcium chloride enhancement method. Freeze-drying refers to the freeze-drying method.  $c = \frac{X_i - X_{mean}}{X_{mean}}$ , where C is the contrast difference, is shown as a percentage.

construct the peripheral nerve and observed the anatomical structure, including the perineurium, epineurium, connective tissue, fascicle, and endoneurium (**Figure 5**). With these 3D fascicular structures, we could proceed to 3D bio-printing.

### Discussion

In this study, we aimed to identify a method for enhancing micro CT images to reconstruct a 3D nerve structure. For PNI, nerve autografting is the gold standard for connecting nerve gaps. However, the procedure has complications, including donor-site dysfunction, excess scarring and a prolonged operation time [20, 21]. Thus, finding substitutes for autografting that have outcomes similar to those of nerve auto-

grafts is a matter of extraordinary significance for patients. In recent decades, 3D biofabrication has been clinically applied in many areas, such as cartilage [22], bioresorbable airway splints [23] and ears [24]. However, these engineered soft tissues are almost entirely biofabricated using a computer-designed model that cannot replicate the original structure of the soft tissue, especially that of peripheral nerves, whose internal structure is very complex. An accurate 3D digital model can be acquired through CT or magnetic resonance imaging, but a high-resolution imaging database is exceedingly difficult to obtain. Micro CT is sensitive enough to create high-resolution images of hard tissue such as bone. However, soft tissue cannot clearly be viewed by micro CT because it has a lower contrast with the background.

## 3D micro CT of the nerve fascicle

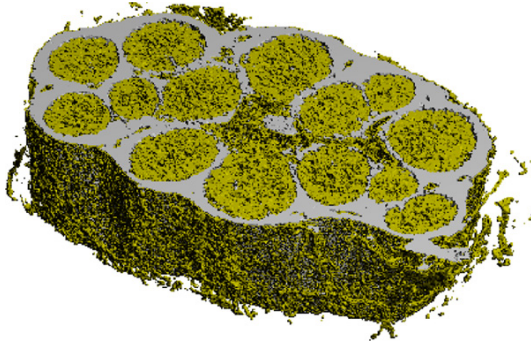


**Figure 5.** A 3D nerve reconstruction created using the calcium chloride method showing normal nerve structures, including the perineurium, epineurium, connective tissue, the fascicle, and the endoneurium.

In this paper, we attempted to outline and evaluate the best method for 3D fascicular structure reconstruction. Our results demonstrated that micro CT surpasses H&E and SEM in reconstructing the 3D microstructure. We then attempted to improve this method. Three techniques, Lugol's iodine solution ( $I_2KI$ ) enhancement, calcium chloride enhancement and freeze-drying, were used to obtain high-resolution 3D images. Comparing the homologous nerve and fascicular structures, we found that the contrast differences were all significantly different ( $P < 0.001$ ) in the calcium chloride-enhanced images, suggesting that this method was the most effective. Thus, the 3D microstructure of a human peripheral nerve was reconstructed using this method. With these data, we could proceed to the 3D bioprinting of nerve grafts.

To the best of our knowledge, this is the first study to demonstrate the use of micro CT to obtain high-quality 3D microstructural peripheral human nerve images using various pretreatment methods. In addition, we identified the best method for reconstructing 3D nerve constructs to bioprint nerves that can replace ANAs for treating PNI. Micro CT is already a useful tool for soft-tissue 3D reconstruction with pretreatments [16, 25]. We used three techniques, i.e., Lugol's iodine solution ( $I_2KI$ ) enhancement, calcium chloride enhancement and freeze-drying, to obtain 3D fascicular images. Iodine-enhanced contrast applied in micro CT scanning has previously been shown to be very useful, particularly in the brain [25], muscle fibers [26], blood vessels [27], and nerves

[28]. To the best of our knowledge, no studies have used iodine-enhanced contrast for micro CT scanning the microstructure of nerves. Some studies have explored the macroscopic and microscopic volume changes in muscles to avoid substantial specimen shrinkage [29]. In our study, we used concentrations of 10%, 20%, and 50% for scanning and determined that the concentration of 50% results in the highest-quality images (**Figure 3A**). We did not consider specimen shrinkage. The mechanisms of iodine staining are not completely understood, but it is clear that the iodine binds to both carbohydrates (e.g., glycogen) and lipids, which are naturally present in varying amounts within many types of soft tissue [19, 30, 31]. From the GVs, we know that the iodine-enhanced method is effective in connective tissue but not in other anatomical structures (**Table 1**).

To the best of our knowledge, saturated calcium chloride is the first micro CT scanning pretreatment to be utilized for nerves. We obtained good images (**Figure 3B**), from which the perineurium, epineurium, connective tissue, and fascicle could be easily distinguished. For the endoneurium, although this method was not superior to freeze-drying, clear images could be obtained. The mechanism of this method is not fully understood, but we know that the CT scanning of bone yields high-quality images because bone contains calcium ions that enhance contrast [14]. If soft tissue is immersed in a calcium ion solution for a sufficiently long time, it undergoes both calcification [32] and osmotic dehydration [33, 34], which can reduce the amount of water in the nerves and improve the nerve micro CT images. The details of the underlying mechanism will be explored in our next study. **Table 1** shows that the GVs of each anatomical structure are distinctive, enabling easy computer recognition for 3D reconstruction.

Freeze-drying methods that can fully retain nerve structures [35, 36], such as fibers and connective tissue, have been identified. These methods are commonly used to keep scaffolds intact in the chemical industry. We applied freeze-drying to micro CT scanning because it can remove water from nerves. However, **Figure 3C** shows that this method cannot enhance contrast with the environment and can distin-

guish the anatomical structure only through tissue density. For the endoneurium, this method can produce clearer images than other methods (**Figure 4**). By calculating the tissue contrast (C), we confirmed that the anatomical structures showed no differences after the freeze-drying method was applied (**Table 1**).

We used the highest-quality image obtained from the calcium chloride method to create a 3D nerve reconstruction (**Figure 5**), which showed a high-quality structure that included the perineurium, epineurium, connective tissue, fascicule, and endoneurium. These 3D data could be used to bioprint nerve grafts. However, our study has limitations, including the following: 1) in testing each method, we did not consider specimen shrinkage; and 2) our micro CT isotropic resolution was not high enough for endoneurium scanning. In future studies, we will focus on these factors and obtain the same macroscopic and microscopic volumes as those of real human nerves at different sites.

The evidence presented suggests that all three methods can be applied to obtain micro CT images for 3D reconstruction and that the resulting images are comparable to H&E and SEM images in showing anatomical structures. However, the best image and GV data for bioprinting can be obtained using the calcium chloride enhancement method.

#### Acknowledgements

This study was supported by grants from the Science and Technology Planning Project of Guangdong Province (No. 2014B050505008), the Natural Science Foundation of Guangdong Province, China (No. S2013010016551, 2015-A030310337), the National Natural Science Foundation of China (No. 81501049, 814-01804), the Medical Scientific Research Foundation of Guangdong Province, China (No. A2015108), the National Basic Research Programme of China (973 Programme, grant No. 2014CB542200), the National High Technology Research and Development Programme of China (863 Programme, No. 2012AA020507), and the National Nonprofit Industry Research Subject (No. 201402016).

#### Disclosure of conflict of interest

None.

**Address correspondence to:** Drs. Xiaolin Liu and Xiang Zhou, Department of Microsurgery and Orthopaedic Trauma, The First Affiliated Hospital of Sun Yat-sen University, 58 Zhongshan Road II, Guangzhou 510080, P. R. China. Tel: +8613600481606; Fax: +86020-87750632; E-mail: gzxiaolinliu@126.com; gzxiaolinliu@hotmail.com (XLL); Tel: +86-15913113047; Fax: +86020-87750632; E-mail: 110337622@qq.com (XZ)

#### References

- [1] Schmidt CE and Leach JB. Neural tissue engineering: strategies for repair and regeneration. *Annu Rev Biomed Eng* 2003; 5: 293-347.
- [2] Pfister BJ, Gordon T, Loverde JR, Kochar AS, Mackinnon SE and Cullen DK. Biomedical engineering strategies for peripheral nerve repair: surgical applications, state of the art, and future challenges. *Crit Rev Biomed Eng* 2011; 39: 81-124.
- [3] Kuffler DP. An assessment of current techniques for inducing axon regeneration and neurological recovery following peripheral nerve trauma. *Prog Neurobiol* 2014; 116: 1-12.
- [4] Kuffler DP. Enhancement of nerve regeneration and recovery by immunosuppressive agents. *Int Rev Neurobiol* 2009; 87: 347-362.
- [5] Hou SY, Zhang HY, Quan DP, Liu XL and Zhu JK. Tissue-engineered peripheral nerve grafting by differentiated bone marrow stromal cells. *Neuroscience* 2006; 140: 101-110.
- [6] Wang D, Liu XL, Zhu JK, Hu J, Jiang L, Zhang Y, Yang LM, Wang HG, Zhu QT, Yi JH and Xi TF. Repairing large radial nerve defects by acellular nerve allografts seeded with autologous bone marrow stromal cells in a monkey model. *J Neurotrauma* 2010; 27: 1935-1943.
- [7] Wang D, Liu XL, Zhu JK, Jiang L, Hu J, Zhang Y, Yang LM, Wang HG and Yi JH. Bridging small-gap peripheral nerve defects using acellular nerve allograft implanted with autologous bone marrow stromal cells in primates. *Brain Res* 2008; 1188: 44-53.
- [8] Murphy SV and Atala A. 3D bioprinting of tissues and organs. *Nat Biotechnol* 2014; 32: 773-785.
- [9] Mironov V, Visconti RP, Kasyanov V, Forgacs G, Drake CJ and Markwald RR. Organ printing: tissue spheroids as building blocks. *Biomaterials* 2009; 30: 2164-2174.
- [10] Norotte C, Marga FS, Niklason LE and Forgacs G. Scaffold-free vascular tissue engineering using bioprinting. *Biomaterials* 2009; 30: 5910-5917.
- [11] Lilje O, Lilje E, Marano AV and Gleason FH. Three dimensional quantification of biological samples using micro-computer aided tomogra-

### 3D micro CT of the nerve fascicle

- phy (micro CT). *J Microbiol Methods* 2013; 92: 33-41.
- [12] Witmer LM. Palaeontology: inside the oldest bird brain. *Nature* 2004; 430: 619-620.
- [13] Neues F and Epple M. X-ray microcomputer tomography for the study of biomineralized endo-and exoskeletons of animals. *Chem Rev* 2008; 108: 4734-4741.
- [14] Burghardt AJ, Issever AS, Schwartz AV, Davis KA, Masharani U, Majumdar S and Link TM. High-resolution peripheral quantitative computed tomographic imaging of cortical and trabecular bone microarchitecture in patients with type 2 diabetes mellitus. *J Clin Endocrinol Metab* 2010; 95: 5045-5055.
- [15] Street J, Bao M, deGuzman L, Bunting S, Peale FV Jr, Ferrara N, Steinmetz H, Hoeffel J, Cleland JL, Daugherty A, van Bruggen N, Redmond HP, Carano RA and Filvaroff EH. Vascular endothelial growth factor stimulates bone repair by promoting angiogenesis and bone turnover. *Proc Natl Acad Sci U S A* 2002; 99: 9656-9661.
- [16] Metscher BD. Micro CT for comparative morphology: simple staining methods allow high-contrast 3D imaging of diverse non-mineralized animal tissues. *BMC Physiol* 2009; 9: 11.
- [17] Xie L, Lin AS, Levenston ME and Guldborg RE. Quantitative assessment of articular cartilage morphology via EPIC- $\mu$ CT. *Osteoarthritis Cartilage* 2009; 17: 313-320.
- [18] Faraj KA, Cuijpers VM, Wismans RG, Walboomers XF, Jansen JA, van Kuppevelt TH and Daamen WF. Micro-computed tomographical imaging of soft biological materials using contrast techniques. *Tissue Eng Part C Methods* 2009; 15: 493-499.
- [19] Gignac PM and Kley NJ. Iodine-enhanced micro-CT imaging: methodological refinements for the study of the soft-tissue anatomy of post-embryonic vertebrates. *J Exp Zool B Mol Dev Evol* 2014; 322: 166-176.
- [20] Moore A, MacEwan M, Santosa K, Chenard K, Ray W, Hunter D, Mackinnon S and Johnson P. Acellular nerve allografts in peripheral nerve regeneration: a comparative study. *Muscle Nerve* 2011; 44: 221-234.
- [21] Stăfănescu O, Jecan R, Bădoiu S, Enescu D and Lascăr I. Peripheral nerve allograft, a reconstructive solution: outcomes and benefits. *Chirurgia* 2012; 107: 438-441.
- [22] Cui X, Breitenkamp K, Finn M, Lotz M and D'Lima D. Direct human cartilage repair using three-dimensional bioprinting technology. *Tissue Eng Part A* 2012; 18: 1304-1312.
- [23] Zopf D, Hollister S, Nelson M, Ohye R and Green G. Bioresorbable airway splint created with a three-dimensional printer. *N Engl J Med* 2013; 368: 2043-2045.
- [24] Lee J, Hong J, Jung J, Shim J, Oh J and Cho D. 3D printing of composite tissue with complex shape applied to ear regeneration. *Biofabrication* 2014; 6: 24103.
- [25] de Crespigny A, Bou-Reslan H, Nishimura MC, Phillips H, Carano RA and D'Arceuil HE. 3D micro-CT imaging of the postmortem brain. *J Neurosci Methods* 2008; 171: 207-213.
- [26] Jeffery NS, Stephenson RS, Gallagher JA, Jarvis JC and Cox PG. Micro-computed tomography with iodine staining resolves the arrangement of muscle fibres. *J Biomech* 2011; 44: 189-192.
- [27] Prajapati SI and Keller C. Contrast enhanced vessel imaging using micro CT. *J Vis Exp* 2011; 47: e2377.
- [28] Hopkins TM, Heilman AM, Liggett JA, LaSance K, Little KJ, Hom DB, Minteer DM, Marra KG and Pixley SK. Combining micro-computed tomography with histology to analyze biomedical implants for peripheral nerve repair. *J Neurosci Methods* 2015; 255: 122-130.
- [29] Vickerton P, Jarvis J and Jeffery N. Concentration-dependent specimen shrinkage in iodine-enhanced micro CT. *J Anat* 2013; 223: 185-193.
- [30] Bock WJ and Shear CR. A staining method for gross dissection of vertebrate muscles. *Anat Anz* 1972; 130: 222-227.
- [31] Metscher BD. Micro CT for developmental biology: a versatile tool for high-contrast 3D imaging at histological resolutions. *Dev Dyn* 2009; 238: 632-640.
- [32] Kim MP, Raho VJ, Mak J and Kaynar AM. Skin and soft tissue necrosis from calcium chloride in a deicer. *J Emerg Med* 2007; 32: 41-44.
- [33] Bai Y, Gao J, Zou DW and Li ZS. Prophylactic octreotide administration does not prevent post-endoscopic retrograde cholangiopancreatography pancreatitis: a meta-analysis of randomized controlled trials. *Pancreas* 2008; 37: 241-246.
- [34] Gerelt B, Ikeuchi Y, Nishiumi T and Suzuki A. Meat tenderization by calcium chloride after osmotic dehydration. *Meat Sci* 2002; 60: 237-244.
- [35] Yu C, Bianco J, Brown C, Fuetterer L, Watkins JF, Samani A and Flynn LE. Porous decellularized adipose tissue foams for soft tissue regeneration. *Biomaterials* 2013; 34: 3290-3302.
- [36] Sridharan R, Reilly RB and Buckley CT. Decellularized grafts with axially aligned channels for peripheral nerve regeneration. *J Mech Behav Biomed Mater* 2015; 41: 124-135.